

Single-step Adversarial training with Dropout Scheduling

Vivek B.S. and R. Venkatesh Babu

Video Analytics Lab, Department of Computational and Data Sciences
Indian Institute of Science, Bangalore, India

Abstract

Deep learning models have shown impressive performance across a spectrum of computer vision applications including medical diagnosis and autonomous driving. One of the major concerns that these models face is their susceptibility to adversarial attacks. Realizing the importance of this issue, more researchers are working towards developing robust models that are less affected by adversarial attacks. Adversarial training method shows promising results in this direction. In adversarial training regime, models are trained with mini-batches augmented with adversarial samples. Fast and simple methods (e.g., single-step gradient ascent) are used for generating adversarial samples, in order to reduce computational complexity. It is shown that models trained using single-step adversarial training method (adversarial samples are generated using non-iterative method) are pseudo robust. Further, this pseudo robustness of models is attributed to the gradient masking effect. However, existing works fail to explain when and why gradient masking effect occurs during single-step adversarial training. In this work, (i) we show that models trained using single-step adversarial training method learn to prevent the generation of single-step adversaries, and this is due to over-fitting of the model during the initial stages of training, and (ii) to mitigate this effect, we propose a single-step adversarial training method with dropout scheduling. Unlike models trained using existing single-step adversarial training methods, models trained using the proposed single-step adversarial training method are robust against both single-step and multi-step adversarial attacks, and the performance is on par with models trained using computationally expensive multi-step adversarial training methods, in white-box and black-box settings.

1. Introduction

Machine learning models are susceptible to adversarial samples: samples with imperceptible, engineered noise designed to manipulate model's output [15, 2, 34, 3, 13, 27]. Further, Szegedy *et al.* [34] observed that these adversarial

samples are transferable across multiple models i.e., adversarial samples generated on one model might mislead other models. Due to which, models deployed in the real world are susceptible to black-box attacks [20, 28], where limited or no knowledge of the deployed model is available to the attacker. Various schemes have been proposed to defend against adversarial attacks (e.g., [13, 29, 23]), in this direction *Adversarial Training (AT)* procedure [13, 35, 22, 40] shows promising results.

In adversarial training regime, models are trained with mini-batches containing adversarial samples typically generated by the model being trained. Adversarial sample generation methods range from simple methods [13] to complex optimization methods [24]. In order to reduce computational complexity, non-iterative methods such as Fast Gradient Sign Method (FGSM) [13] are typically used for generating adversarial samples. Further, it has been shown that models trained using single-step adversarial training methods are pseudo robust [35]:

- Although these models appears to be robust to single-step attacks in white-box setting (complete knowledge of the deployed model is available to the attacker), they are susceptible to single-step attacks (non-iterative methods) in black-box attack setting [35].
- Further, these models are susceptible to multi-step attacks (iterative methods) in both white-box setting [18] and black-box setting [10].

Tramer *et al.* [35] demonstrated that models trained using single-step adversarial training method converges to degenerative minima, and exhibit *gradient masking effect*. Single-step adversarial sample generation methods such as FGSM, compute adversarial perturbations based on the linear approximation of the model's loss function i.e., image is perturbed in the direction of the gradient of loss with respect to the input image. Gradient masking effect causes this linear approximation of loss function to become unreliable for generating adversarial samples during single-step adversarial training. Madry *et al.* [22] demonstrated that models trained using adversarial samples that maximize the training loss are robust against single-step and multi-step at-

tacks. Such samples could be generated using the Projected Gradient Descent (PGD). However, PGD method is an iterative method, due to which training time increases substantially. Though prior works have enabled to learn robust models, they fail to answer the following important questions: (i) *Why models trained using single-step adversarial training method exhibit gradient masking effect?* and (ii) *At what phase of the single-step adversarial training, the model starts to exhibit gradient masking effect?*

In this work, we attempt to answer these questions and propose a novel single-step adversarial training method to learn robust models. First, we show that models trained using single-step adversarial training method learn to prevent the generation of single-step adversaries, and this is due to over-fitting of the model during the initial stages of training. Over-fitting of the model on single-step adversaries causes linear approximation of loss function to become unreliable for generating adversarial samples i.e., gradient masking effect. Finally, we propose a single-step adversarial training method with dropout scheduling to learn robust models. Note that, just adding dropout layer (typical setting: dropout layer with fixed dropout probability after FC+ReLU layer) does not help the model trained using single-step adversarial training method to gain robustness. Prior works observed no significant improvement in the robustness of models (with dropout layers in typical setting), trained using normal training and single-step adversarial training methods [13, 18]. Results for these settings are shown in section 4.1. Unlike typical setting, we introduce dropout layer after each non-linear layer (i.e., dropout-2D after conv2D+ReLU, and dropout-1D after FC+ReLU) of the model, and further decay its dropout probability as training progress. Interestingly, we show that this proposed dropout setting has significant impact on the model’s robustness. The major contributions of this work can be listed as follows:

- We show that models trained using single-step adversarial training method learns to prevent the generation of single-step adversaries, and this is due to over-fitting of the model during the initial stages of training.
- Harnessing on the above observation, we propose a single-step adversarial training method with dropout probability scheduling. Unlike models trained using existing single-step adversarial training methods, models trained using the proposed method are robust against both single-step and multi-step attacks.
- The proposed single-step adversarial training method is much faster than multi-step adversarial training methods, and achieves on par results.

2. Notations

Consider a neural network f trained to perform image classification task, and θ represents parameters of the neural network. Let x represents the image from the dataset and y_{true} be its corresponding ground truth label. The neural network is trained using loss function J (e.g., cross-entropy loss), and $\nabla_x J$ represents the gradient of loss with respect to the input image x . Adversarial image x_{adv} is generated by adding norm-bounded perturbation δ to the image x . Perturbation size (ϵ) represents the l_∞ norm constraint on the generated adversarial perturbation i.e., $\|\delta\|_\infty \leq \epsilon$. Please refer to supplementary document for details on adversarial training and attack generation methods.

3. Related Works

Following the findings of Szegedy *et al.* [34], various attacks (e.g., [13, 24, 8, 26, 25, 10, 12]) have been proposed. Further, in order to defend against adversarial attacks, various schemes such as adversarial training (e.g., [13, 18, 22, 40, 5, 4]) and input pre-processing (e.g., [14, 31]) have been proposed. Athalye *et al.* [1] showed that obfuscated gradients give a false sense of robustness, and broke seven out of nine defense papers [6, 21, 14, 38, 32, 31, 22, 21, 9] accepted to ICLR 2018. In this direction, adversarial training method [22], shows promising results for learning robust deep learning models. Kurakin *et al.* [18] observed that models trained using single-step adversarial training methods are susceptible to multi-step attacks. Further, Tramer *et al.* [35] demonstrated that these models exhibit gradient masking effect, and proposed Ensemble Adversarial Training (EAT) method. However, models trained using EAT are still susceptible to multi-step attacks in white-box setting. Madry *et al.* [22] demonstrated that adversarially trained model can be made robust against white-box attacks, if perturbation crafted while training maximizes the loss. Zhang *et al.* [40] proposed a regularizer for multi-step adversarial training, that encourages the output of the network to be smooth. On the other hand, works such as [30] and [36] propose a method to learn models that are provably robust against norm bounded adversarial attacks. However, scaling these methods to deep networks and large perturbation sizes is difficult. Whereas, in this work we show that it is possible to learn robust models using single-step adversarial training method, if over-fitting of the model on adversarial samples is prevented during training. We achieve this by introducing dropout layer after each non-linear layer of the model with a dropout schedule.

4. Over-fitting and its effect during adversarial training

In this section, we show that models trained using single-step adversarial training method learn to prevent the genera-

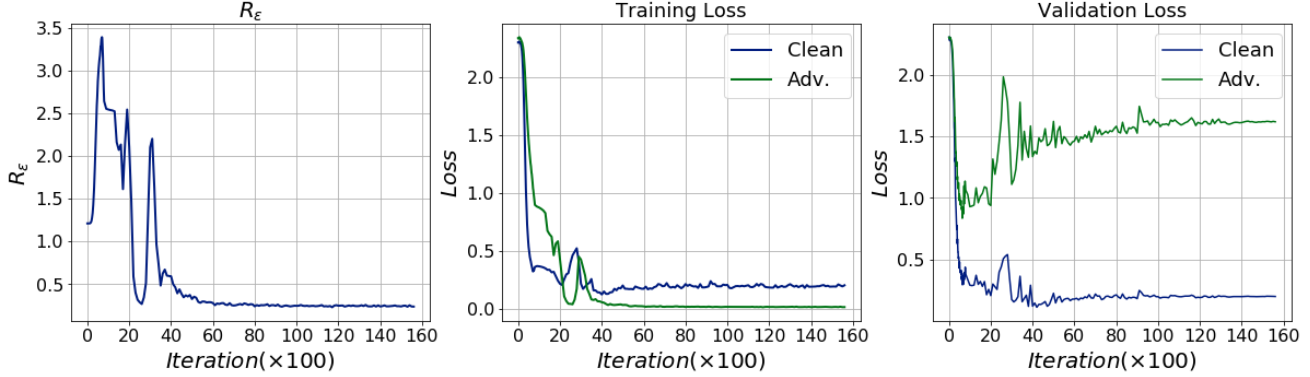


Figure 1: **Single-step adversarial training:** Trend of R_ϵ , training loss, and validation loss during single-step adversarial training, obtained for LeNet+ trained on MNIST dataset. Column-1: plot of R_ϵ versus training iteration. Column-2: training loss versus training iteration. Column-3: validation loss versus training iteration. Note that, when R_ϵ starts to decay, loss on adversarial validation set starts to increase indicating that the model is over-fitting on the adversarial samples.

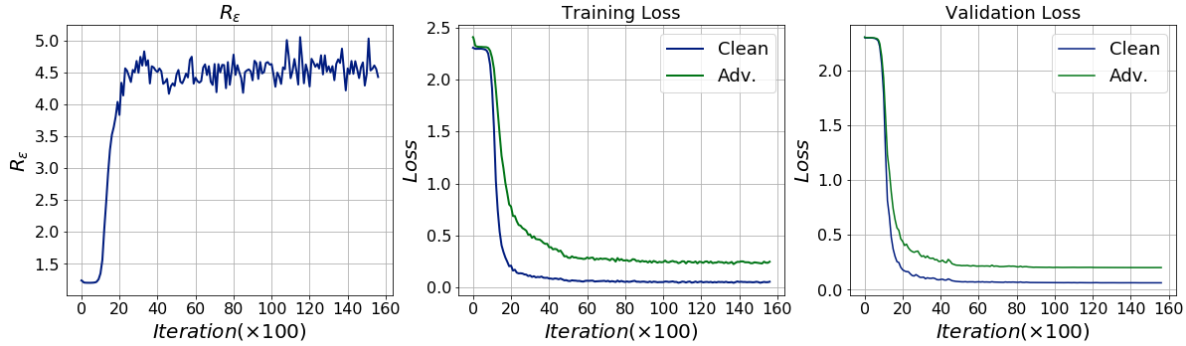


Figure 2: **Multi-step adversarial training:** Trend of R_ϵ , training loss, and validation loss during multi-step adversarial training, obtained for LeNet+ trained on MNIST dataset. Column-1: plot of R_ϵ versus training iteration. Column-2: training loss versus training iteration. Column-3: validation loss versus training iteration. Note that, for the entire training duration R_ϵ does not decay, and no over-fitting effect can be observed.

tion of single-step adversaries, and this is due to over-fitting of the model during the initial stages of training. First, we discuss the criteria for learning robust models using adversarial training method, and then we show that this criteria is not satisfied during single-step adversarial training method. Most importantly, we show that over-fitting effect is the reason for failure to satisfy the criteria.

Madry *et al.* [22] demonstrated that it is possible to learn robust models using adversarial training method, if adversarial perturbations (l_∞ norm bounded) crafted while training maximizes the model’s loss. This training objective is formulated as a minimax optimization problem (Eq. 1). Where ψ represents the feasible set e.g., for l_∞ norm constraint attacks $\psi = \{\delta : \|\delta\|_\infty \leq \epsilon\}$, and D is the training set.

$$\min_{\theta} \left[E_{(x,y) \in D} \left[\max_{\delta \in \psi} J(f(x + \delta; \theta), y_{true}) \right] \right] \quad (1)$$

$$R_\epsilon = \frac{loss_{adv}}{loss_{clean}} \quad (2)$$

At each iteration, norm bounded adversarial perturbations that maximizes the training loss should be generated. Further, the model’s parameters (θ) should be updated so as to decrease the loss on such adversarial samples. Madry *et al.* [22] solves the maximization step by generating adversarial samples using an iterative method named Projected Gradient Descent (PGD). In order to quantify the extent of inner maximization of Eq. (1), we compute loss ratio R_ϵ using Eq. (2). Loss ratio is defined as the ratio of loss on the adversarial samples to the loss on its corresponding clean samples for a given perturbation size ϵ . The metric R_ϵ captures the extent of inner maximization achieved by the generated adversarial samples i.e., factor by which loss has increased by perturbing the clean samples.

A sample is said to be an adversarial sample if it is capable of manipulating the model’s prediction. Such manipulations could be achieved by perturbing the samples along the adversarial direction [13]. A perturbation is said to be an *adversarial perturbation* when it causes loss on the perturbed sample to increase. This implies that the loss

on the adversarially perturbed samples should be greater than the loss on the corresponding unperturbed samples i.e., $loss_{adv} > loss_{clean}$. Based on these facts, R_ϵ can be interpreted in the following manner:

- Generated perturbation is said to be an *adversarial perturbation* if $R_\epsilon > 1$ i.e., $loss_{adv} > loss_{clean}$
- $R_\epsilon < 1$ i.e., $loss_{adv} < loss_{clean}$, implies that the generated perturbation is not an adversarial perturbation. The attack method fails to generate *adversarial perturbations* for the given model.

We obtain the plot of R_ϵ versus iteration for models trained using single-step adversarial training method [13] and multi-step adversarial training method [22]. Column-1 of Fig. 1 and Fig. 2 show these plots obtained for LeNet+ trained on MNIST dataset [19] using single-step and multi-step adversarial training methods respectively. It can be observed that during single-step adversarial training, R_ϵ initially increases and then starts to decay rapidly. Further R_ϵ becomes less than one after 20 ($\times 100$) iterations. This implies that single-step adversarial sample generation method is unable to generate *adversarial perturbations* for the model, leading to adversarial training without useful adversarial samples.

We demonstrate this behavior of the model to prevent the inclusion of adversarial samples is due to over-fitting on the adversarial samples. Typically during normal training, loss on the validation set is monitored to detect over-fitting effect i.e., validation loss increases when the model starts to over-fit on the training set. Unlike normal training, during adversarial training we monitor the loss on the clean and adversarial validation set. A normally trained model is used for generating adversarial validation set, so as to ensure that the generated adversarial validation samples are independent of the model being trained. Column-2 and column-3 of Fig. 1 shows the plot of loss versus iteration during training of LeNet+ on MNIST dataset using single-step adversarial training. It can be observed that, when R_ϵ starts to decay, loss on the adversarial validation set starts to increase. This increase in the validation loss indicates over-fitting of the model on the single-step adversaries. Whereas, during multi-step adversarial training method, R_ϵ initially increases and then saturates (column-1, Fig. 2). Further, no such over-fitting effect is observed for the entire training duration (column-3, Fig. 2). Note that, a normally trained model was used for generating FGSM ($\epsilon=0.3$) adversarial validation set, and we observe similar trend if a normally trained model of different architecture is used for generating FGSM adversarial validation set, please refer to supplementary document.

4.1. Effect of dropout layer

In the previous section, we showed that models trained using single-step adversarial training learn to prevent the generation of single-step adversaries. Further, we demonstrated that this behavior of models is due to over-fitting. Dropout layer [33] has been shown to be effective in mitigating over-fitting during training, and typically dropout-1D layer is added after FC+ReLU layers in the networks. We refer to this setting as *typical setting*. Prior works which used dropout layer during single-step adversarial training observed no significant improvement in the model’s robustness. This is due to the use of dropout layer in *typical setting*. Whereas, we empirically show that it is necessary to introduce dropout layer after every non-linear layer of the model (*proposed dropout setting* i.e., dropout-2D after Conv2D+ReLU layer and dropout-1D after FC+ReLU layer) to mitigate over-fitting during single-step adversarial training, and to enable the model to gain robustness against adversarial attacks (single-step and multi-step attacks). We train LeNet+ with dropout layer in *typical setting* and in the *proposed setting* respectively, on MNIST dataset using single-step adversarial training method for different values of dropout probability. After training, we obtain the performance of these resultant models against PGD attack ($\epsilon=0.3$, $\epsilon_{step}=0.01$, $steps=40$). Column-1 of Fig. 3 shows the trend of accuracy of these models for PGD attack with respect to the dropout probability used while training. It can be observed that the gain in the robustness of adversarially trained model with dropout layer in the proposed setting is significantly better compared to the adversarially trained model with dropout layer in typical setting (FAT-TS). From column-2 of Fig. 3, it can be observed that the robustness of adversarially trained model with dropout layer in the proposed setting, increases with the increase in the dropout probability (p) and reaches a peak value at $p=0.4$. Further increase in the dropout probability causes decrease in the accuracy on both clean and adversarial samples. Based on this observation, we propose an improved single-step adversarial training in the next subsection. Furthermore, we perform normal training of LeNet+ with dropout layers in typical setting and in the proposed setting, on MNIST dataset. From column-1 of Fig. 3, it can be observed that there is no significant improvement in the robustness of these normally trained models.

4.2. SADS: Single-step Adversarial training with Dropout Scheduling

Column-1 of Fig. 3 indicates that use of dropout layer in typical setting is not sufficient to avoid over-fitting on adversarial samples, and we need severe dropout regime involving all the layers (i.e., proposed setting: dropout layer after Conv2D+ReLU and FC+ReLU layers) of the network in order to avoid over-fitting. For the proposed dropout regime,

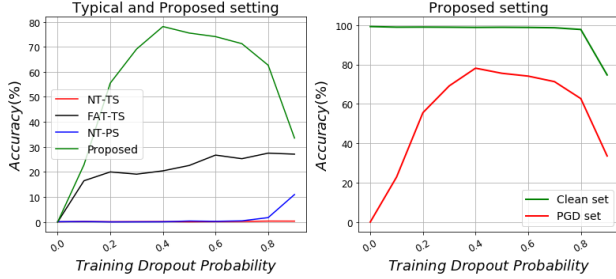


Figure 3: **Column-1:** Effect of dropout probability of dropout layers in typical setting and in the proposed setting on the model’s robustness against PGD attack ($\epsilon=0.3$, $\epsilon_{step}=0.01$ and $steps=40$). Obtained for LeNet+ trained on MNIST dataset. NT-TS: Normal training with dropout layer in typical setting. FAT-TS: Single-step adversarial training with dropout layer in typical setting. NT-PS: Normal training with dropout layer in the proposed setting. Proposed: Single-step adversarial training with dropout layer in the proposed setting. **Column-2:** Effect of dropout probability on the model’s accuracy on clean and PGD adversarial validation set ($\epsilon=0.3$, $\epsilon_{step}=0.01$ and $steps=40$). Obtained for LeNet+ with dropout layer in the proposed setting, trained using single-step adversarial training method on MNIST dataset.

determining exact dropout probability is network dependent and is difficult. Further, having high dropout probability causes under-fitting of the model, and having low dropout probability causes the model to over-fit on the adversarial samples.

Based on these observations, we propose a single-step adversarial training method with dropout scheduling (Algorithm 1). In the proposed training method, we introduce dropout layer after each non-linear layer of the model to be trained. We initialize these dropout layers with a high dropout probability P_d . Further, during training we linearly decay the dropout probability of all the dropout layers and this decay in the dropout probability is controlled by the hyper-parameter r_d . The hyper-parameter, r_d is expressed in terms of maximum training iterations (e.g., $r_d=1/2$ implies that dropout probability reaches zero when the current training iteration is equal to half of the maximum training iterations). In experimental section 5, we show the effectiveness of the proposed training method. Note that dropout layer is only used while training.

5. Experiments

In this section, we show the effectiveness of models trained using the proposed single-step adversarial training method (SADS) in white-box and black-box settings. We perform the sanity tests described in [7], in order to verify that models trained using SADS are robust and

Algorithm 1: Single-step Adversarial training with Dropout Scheduling (SADS)

Input:

- Training mini-batch size (m)
- Maximum training iterations ($Max_{iteration}$)
- Hyper-parameters: P_d, r_d

1 Initialization

Randomly initialize network N

$iteration = 0$

$prob = P_d$

Insert dropout layer after each non-linear layer of the network N

Set dropout probability (p) of all the dropout layers with $prob$

while $iteration \leq Max_{iteration}$ **do**

2 Read minibatch $B=\{x^1, \dots, x^m\}$ from training set

3 Compute FGSM adversarial sample

$\{x^1_{adv}, \dots, x^m_{adv}\}$ from corresponding clean samples $\{x^1, \dots, x^m\}$ using the current state of the network N

4 Make new minibatch $B^* = \{x^1_{adv}, \dots, x^m_{adv}\}$
/*Forward pass, compute loss, backward pass, and update parameters*/

5 Do one training step of Network N using minibatch B^*

/*Update dropout probability of Dropout-1D and Dropout-2D layers with $prob^*$ */

6 $prob = \max(0, P_d \cdot (1 - \frac{iteration}{r_d \cdot Max_{iteration}}))$

7 $iteration = iteration + 1$

8 end

does not exhibit *obfuscated gradients* (Athalye *et al.* [1] demonstrated that models exhibiting obfuscated gradients are not robust against adversarial attacks). We show results on MNIST [19], Fashion-MNIST [37] and CIFAR-10 [16] datasets. We use LeNet+ (please refer to supplementary document for details on network architecture) for both MNIST and Fashion-MNIST datasets. For CIFAR-10 dataset, WideResNet-28-10 [39] is used. These models are trained using SGD with momentum. Step-policy is used for learning rate scheduling. For all datasets, images are pre-processed to be in $[0,1]$ range. For CIFAR-10, random crop and horizontal flip are performed for data-augmentation.

Evaluation: We show the performance of models against adversarial attacks in white-box and black-box setting. For SADS, we report mean and standard deviation over three runs.

Attacks: For l_∞ based attacks, we use Fast Gradient Sign Method (FGSM) [13], Iterative Fast Gradient Sign Method (IFGSM) [17], Momentum Iterative Fast Gradient Sign Method (MI-FGSM) [10] and Projected Gradient Descent

Table 1: **MNIST: White-Box setting.** Classification accuracy (%) of models trained on MNIST dataset using different training methods. For all attacks $\epsilon=0.3$ is used and for PGD attack $\epsilon_{step}=0.01$ is used. For both IFGSM and PGD attacks, steps is set to 40.

Training Method	Clean	Attack Method		
		FGSM	IFGSM	PGD
NT	99.24	11.65	0.31	0.01
Multi-step adversarial training				
PAT	98.41	95.56	92.64	92.08
TRADES	98.70	96.30	95.14	95.05
Single-step adversarial training				
FAT	99.34	89.04	1.19	0.17
SADS	98.89	94.78	89.35	88.51
	± 0.01	± 0.19	± 0.09	± 0.22

Table 2: **Fashion-MNIST: White-Box attack.** Classification accuracy (%) of models trained on Fashion-MNIST dataset using different training methods. For all attacks $\epsilon=0.1$ is used and for PGD attack $\epsilon_{step}=0.01$ is used. For both IFGSM and PGD attacks, steps is set to 40.

Training Method	Clean	Attack Method		
		FGSM	IFGSM	PGD
NT	91.42	6.46	1.01	0.16
Multi-step adversarial training				
PAT	84.55	77.30	75.95	75.18
TRADES	86.69	80.39	78.94	78.04
Single-step adversarial training				
FAT	90.45	83.43	21.26	16.65
SADS	85.21	75.81	71.14	69.51
	± 0.08	± 1.31	± 1.01	± 1.43

(PGD) [22]. For l_2 based attack, we use DeepFool [24] and Carlini & Wagner [8].

Perturbation size: For l_∞ based attacks, we set perturbation size (ϵ) to the values described in [22] i.e., $\epsilon=0.3$, 0.1 and 8/255 for MNIST, Fashion-MNIST and CIFAR-10 datasets respectively.

Comparisons: We compare the performance of the proposed single-step adversarial training method (SADS) with Normal training (NT), FGSM adversarial training (FAT) [18], Ensemble adversarial training (EAT) [35], PGD adversarial training (PAT) [22], and TRADES [40]. Note that, FAT, EAT and SADS (ours) are single-step adversarial training methods, whereas PAT and TRADES are multi-step adversarial training methods. Results for EAT are shown in supplementary document.

Table 3: **CIFAR-10: White-Box attack.** Classification accuracy (%) of models trained on CIFAR-10 dataset using different training methods. For all attacks $\epsilon=8/255$ is used and for PGD attack $\epsilon_{step}=2/255$ is used. For both IFGSM and PGD attacks, steps is set to 7.

Training Method	Clean	Attack Method		
		FGSM	IFGSM	PGD
NT	94.75	28.16	0.07	0.03
Multi-step adversarial training				
PAT	85.70	53.96	48.65	47.23
TRADES	87.20	56.34	51.21	50.03
Single-step adversarial training				
FAT	94.04	98.54	0.31	0.09
SADS	82.01	51.99	46.37	45.66
	± 0.06	± 1.02	± 1.17	± 1.26

5.1. Performance in White-box setting

We train models on MNIST, Fashion-MNIST and CIFAR-10 datasets respectively, using NT, FAT, PAT, TRADES and SADS (Algorithm 1) training methods. Models are trained for 50, 50 and 100 epochs on MNIST, Fashion-MNIST and CIFAR-10 datasets respectively. For SADS, we set the hyper-parameter P_d and r_d to (0.8, 0.5), (0.8, 0.75) and (0.5, 0.5) for MNIST, Fashion-MNIST and CIFAR-10 datasets respectively. Table 1, 2 and 3 shows the performance of these models against single-step and multi-step attacks in white-box setting, rows represent the training method and columns represent the attack generation method. It can be observed that models trained using FAT are not robust against multi-step attacks. Whereas, models trained using PAT, TRADES and SADS are robust against both single-step and multi-step attacks. Unlike PAT and TRADES, the proposed SADS method is a single-step adversarial training method.

PGD attack with large steps: Engstrom *et al.* [11] demonstrated that the performance of models trained using certain adversarial training methods degrade significantly with increase in the number of steps of PGD attack. In order to verify that such behavior is not observed in models trained using SADS, we obtain the plot of classification accuracy on PGD test-set versus steps of PGD attack. Fig. 4 shows these plots obtained for models trained using PAT and SADS on MNIST, Fashion-MNIST and CIFAR-10 datasets respectively. It can be observed that the accuracy of models on PGD test set initially decreases slightly and then saturates. Even for PGD attack with large steps, there is no significant degradation in the performance of models trained using PAT and SADS methods. In supplementary document, we show the effect of hyper-parameters of the proposed training method.

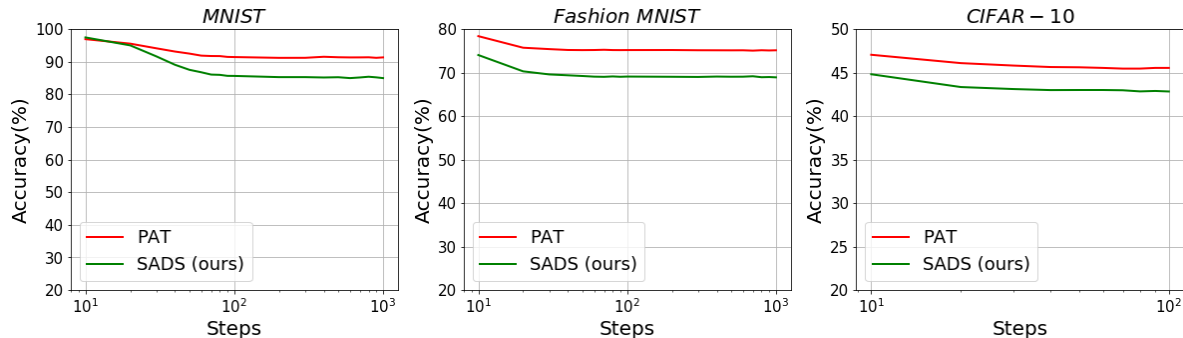


Figure 4: Plot of accuracy of the model trained using PAT and SADS, on PGD adversarial test set versus steps of PGD attack with fixed ϵ . For PGD attack we set $(\epsilon, \epsilon_{step})$ to $(0.3, 0.01)$, $(0.1, 0.01)$ and $(8/255, 2/255)$ for MNIST, Fashion-MNIST and CIFAR-10 datasets. Note, x -axis is in logarithmic scale.

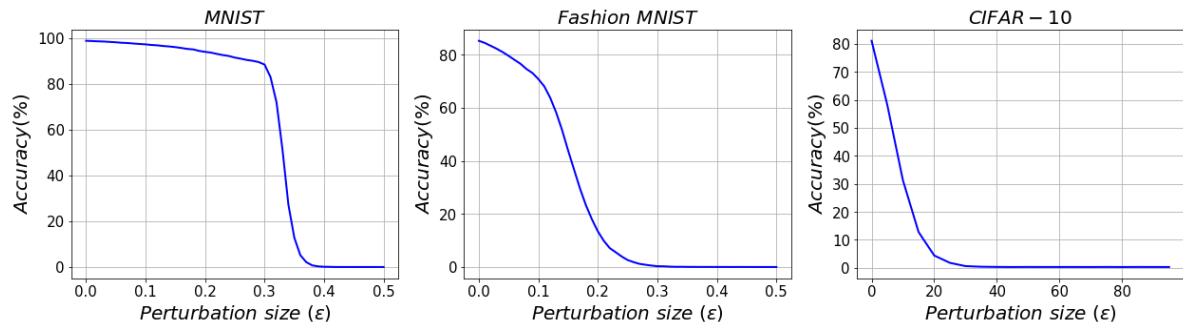


Figure 5: Plot of accuracy versus perturbation size of PGD attack, obtained for models trained using SADS. It can be observed that the accuracy of the model is zero for PGD attack with large perturbation size.

Table 4: Black-box setting: Performance of models trained on MNIST, Fashion-MNIST and CIFAR-10 datasets using different training method, against adversarial attacks in black-box setting. Source models are used for generating adversarial samples, and the target models are tested on these generated adversarial samples.

MNIST					
Source Model		Target Model			
		NT	FAT	PAT	SADS
Model-A	FGSM ($\epsilon=0.3$)	29.09	79.49	96.01	95.06
	MI-FGSM ($\epsilon=0.3$, steps=40)	10.69	72.44	95.83	94.80
Model-B	FGSM ($\epsilon=0.3$)	28.13	72.39	96.15	95.11
	MI-FGSM ($\epsilon=0.3$, steps=40)	12.32	70.79	95.97	94.81
Fashion-MNIST					
Model-A	FGSM ($\epsilon=0.1$)	36.66	88.26	81.32	80.86
	MI-FGSM ($\epsilon=0.1$, steps=40)	33.04	88.36	81.20	80.68
Model-B	FGSM ($\epsilon=0.1$)	39.03	85.40	80.01	78.94
	MI-FGSM ($\epsilon=0.1$, steps=40)	38.01	84.72	79.84	78.59
CIFAR-10					
VGG-11	FGSM ($\epsilon=8/255$)	48.46	78.70	78.12	77.97
	MI-FGSM ($\epsilon=8/255$, steps=7)	31.61	76.35	78.36	77.95
DenseNet-BC-100	FGSM ($\epsilon=8/255$)	39.58	86.90	80.29	80.06
	MI-FGSM ($\epsilon=8/255$, steps=7)	28.50	86.42	80.42	80.28

5.2. Performance in Black-box setting

In this subsection, we show the performance of models trained using different training methods against adversarial

attacks in black-box setting. Typically, a substitute model (source model) is trained on the same task using normal training method, and this trained substitute model is used for generating adversarial samples. The generated adversarial samples are transferred to the deployed model (target model). We use FGSM and MI-FGSM methods for generating adversarial samples, since samples generated using these methods show good transfer rates [10]. Table 4 shows the performance of models trained using different methods, in black-box setting. It can be observed that the performance of models trained using PAT and SADS in black-box setting is better than that in white-box setting. Further, it can be observed that the performance of models trained on MNIST and CIFAR-10 datasets using FAT is worse in black-box setting than compared in white-box setting. Please refer to supplementary file for details on network architecture of source models.

5.3. Performance against DeepFool and C&W attacks

DeepFool [24] and C&W [8] attacks generate adversarial perturbations with minimum l_2 norm, that is required to fool the classifier. These methods measure the robustness of the model in terms of the average l_2 norm of the generated adversarial perturbations for the test set. For an undefended model, adversarial perturbation with small l_2 norm

Table 5: **DeepFool and C&W attacks:** Performance of models trained using different training methods against DeepFool and C&W attacks. These attack methods measure the robustness of the model based on the average l_2 norm of the generated perturbations, higher the better. Success defines the percentage of samples of test set that has been misclassified. Note that, for models trained using PAT and SADS, perturbations with relatively large l_2 norm is required to fool the classifier.

Method	MNIST				F-MNIST				CIFAR-10			
	DeepFool		CW		DeepFool		CW		DeepFool		CW	
	Success	Mean l_2	Success	Mean l_2	Success	Mean l_2	Success	Mean l_2	Success	Mean l_2	Success	Mean l_2
NT	99.35	1.837	100	1.659	93.73	0.796	100	0.709	96	0.20	100	0.12
FAT	99.37	1.455	100	0.798	93.11	1.514	100	1.167	96	0.25	100	0.10
PAT	85.68	4.633	99	2.779	90.29	2.635	100	1.572	92	1.22	100	0.88
SADS	95.89	3.692	100	2.321	90.68	2.305	100	1.308	93	0.97	100	0.71
	± 0.06	± 0.033	$0 \pm$	± 0.027	± 0.26	± 0.102	± 0	± 0.188	± 0.32	± 0.043	± 0	± 0.014

Table 6: Comparison of training time per epoch of models trained on MNIST and CIFAR-10 datasets respectively, obtained for different training methods.

Method	Training time per epoch (sec.)	
	MNIST	CIFAR-10
NT	~ 2.7	~ 104
FAT	~ 4.1	~ 159
PAT	~ 53	~ 820
TRADES	~ 104	~ 1558
SADS	~ 4.3	~ 187

is enough to fool the classifier. Whereas for robust models, adversarial perturbation with relatively large l_2 norm is required to fool the classifier. Table 5, shows the performance of models trained using NT, FAT, PAT and SADS methods, against DeepFool and C&W attacks. It can be observed that models trained using PAT and SADS have relatively large average l_2 norm. Whereas, for models trained using NT and FAT have small average l_2 norm.

5.4. Sanity tests

We perform sanity tests described in [7] to verify whether models trained using SADS are adversarially robust and are not exhibiting obfuscated gradients. We perform following sanity tests:

- *Iterative attacks should perform better than non-iterative attacks*
- *White-box attacks should perform better than black-box attacks*
- *Unbounded attacks should reach 100% success*
- *Increasing distortion bound should increase attack success rate*

Models trained using SADS pass above tests. From table 1, 2 and 3, it can be observed that iterative attacks (IFGSM and PGD) are stronger than non-iterative attack (FGSM) for models trained using SADS. Comparing results in Tables 1, 2 and 3 with results in Table 4, it can be observed that white-box attacks are stronger than black-box

attacks for models trained using SADS. Fig. 5 shows the accuracy plot for the model on test set versus perturbation size of PGD attack, obtained for models trained using SADS. It can be observed that the model’s accuracy falls to zero for large perturbation size (ϵ). From Fig. 5, it can be observed that PGD attack success rate (attack success rate is equal to $(100 - \text{model’s accuracy})\%$) increases with increase in the distortion bound (perturbation size) of the attack.

5.5. Time Complexity

In order to quantify the complexity of different training methods, we measure training time per epoch (seconds) for models trained using different training methods. Table 6 shows the training time per epoch for models trained on MNIST and CIFAR-10 datasets respectively. Note that the training time of SADS and FAT is of the same order. The increase in the training time for PAT and TRADES is due to their iterative nature of generating adversarial samples. We ran this timing experiment on a machine with NVIDIA Titan Xp GPU, with no other jobs on this GPU.

6. Conclusion

In this work, we have demonstrated that models trained using single-step adversarial training methods learn to prevent the generation of adversaries due to over-fitting of the model during the initial stages of training. To mitigate this effect, we have proposed a novel single-step adversarial training method with dropout scheduling. Unlike existing single-step adversarial training methods, models trained using the proposed method achieves robustness not only against single-step attacks but also against multi-step attacks. Further, the performance of models trained using the proposed method is on par with models trained using multi-step adversarial training methods, and is much faster than multi-step adversarial training methods.

Acknowledgment: This work was supported by Uchatar Avishkar Yojana (UAY) project (IISC_010), MHRD, Govt. of India.

References

- [1] Anish Athalye, Nicholas Carlini, and David Wagner. Obfuscated Gradients Give a False Sense of Security: Circumventing Defenses to Adversarial Examples. In *International Conference on Machine Learning (ICML)*, 2018. [2](#), [5](#)
- [2] Battista Biggio, Iginio Corona, Davide Maiorca, Blaine Nelson, Nedim Šrđić, Pavel Laskov, Giorgio Giacinto, and Fabio Roli. Evasion attacks against machine learning at test time. In *Joint European Conference on Machine Learning and Knowledge Discovery in Databases*, 2013. [1](#)
- [3] Battista Biggio, Giorgio Fumera, and Fabio Roli. Pattern recognition systems under attack: Design issues and research challenges. *International Journal of Pattern Recognition and Artificial Intelligence*, 28(07), 2014. [1](#)
- [4] Vivek B.S., Arya Baburaj, and R. Venkatesh Babu. Regularizer to mitigate gradient masking effect during single-step adversarial training. In *IEEE Conference on Computer Vision and Pattern Recognition Workshops (CVPRW)*, 2019. [2](#)
- [5] Vivek B.S., Konda Reddy Mopuri, and R. Venkatesh Babu. Gray-box adversarial training. In *European Conference on Computer Vision (ECCV)*, 2018. [2](#)
- [6] Jacob Buckman, Aurko Roy, Colin Raffel, and Ian Goodfellow. Thermometer Encoding: One Hot Way To Resist Adversarial Examples. In *International Conference on Learning Representations (ICLR)*, 2018. [2](#)
- [7] Nicholas Carlini, Anish Athalye, Nicolas Papernot, Wieland Brendel, Jonas Rauber, Dimitris Tsipras, Ian Goodfellow, and Aleksander Madry. On evaluating adversarial robustness. *arXiv preprint arXiv:1902.06705*, 2019. [5](#), [8](#)
- [8] Nicholas Carlini and David Wagner. Towards Evaluating the Robustness of Neural Networks. *arXiv preprint arXiv:1608.04644*, 2016. [2](#), [6](#), [7](#)
- [9] Guneet S. Dhillon, Kamyar Aizzadenesheli, Jeremy D. Bernstein, Jean Kossaifi, Aran Khanna, Zachary C. Lipton, and Animashree Anandkumar. Stochastic activation pruning for robust adversarial defense. In *International Conference on Learning Representations (ICLR)*, 2018. [2](#)
- [10] Yinpeng Dong, Fangzhou Liao, Tianyu Pang, Hang Su, Jun Zhu, Xiaolin Hu, and Jianguo Li. Boosting adversarial attacks with momentum. In *IEEE Conference on Computer Vision and Pattern Recognition (CVPR)*, 2018. [1](#), [2](#), [5](#), [7](#), [11](#)
- [11] Logan Engstrom, Andrew Ilyas, and Anish Athalye. Evaluating and understanding the robustness of adversarial logit pairing. *arXiv preprint arXiv:1807.10272*, 2018. [6](#)
- [12] Aditya Ganeshan, Vivek B.S., and R. Venkatesh Babu. FDA: Feature Disruptive Attack. In *IEEE International Conference on Computer Vision (ICCV)*, 2019. [2](#)
- [13] Ian J. Goodfellow, Jonathon Shlens, and Christian Szegedy. Explaining and Harnessing Adversarial Examples. In *International Conference on Learning Representations (ICLR)*, 2015. [1](#), [2](#), [3](#), [4](#), [5](#), [11](#)
- [14] Chuan Guo, Mayank Rana, Moustapha Cisse, and Laurens van der Maaten. Countering Adversarial Images using Input Transformations. In *International Conference on Learning Representations (ICLR)*, 2018. [2](#)
- [15] Ling Huang, Anthony D. Joseph, Blaine Nelson, Benjamin I.P. Rubinstein, and J. D. Tygar. Adversarial Machine Learning. In *ACM Workshop on Security and Artificial Intelligence, AISec*, 2011. [1](#)
- [16] Alex Krizhevsky, Vinod Nair, and Geoffrey Hinton. Cifar-10 (canadian institute for advanced research). [5](#), [13](#)
- [17] Alexey Kurakin, Ian Goodfellow, and Samy Bengio. Adversarial examples in the physical world. *arXiv preprint arXiv:1607.02533*, 2016. [5](#), [11](#)
- [18] Alexey Kurakin, Ian J. Goodfellow, and Samy Bengio. Adversarial Machine Learning at Scale. In *International Conference on Learning Representations (ICLR)*, 2017. [1](#), [2](#), [6](#)
- [19] Yann LeCun. The mnist database of handwritten digits. <http://yann.lecun.com/exdb/mnist/>. [4](#), [5](#)
- [20] Yanpei Liu, Xinyun Chen, Chang Liu, and Dawn Song. Delving into transferable adversarial examples and black-box attacks. In *International Conference on Learning Representations (ICLR)*, 2017. [1](#)
- [21] Xingjun Ma, Bo Li, Yisen Wang, Sarah M. Erfani, Sudanthi Wijewickrema, Grant Schoenebeck, Michael E. Houle, Dawn Song, and James Bailey. Characterizing Adversarial Subspaces Using Local Intrinsic Dimensionality. In *International Conference on Learning Representations (ICLR)*, 2018. [2](#)
- [22] Aleksander Madry, Aleksandar Makelov, Ludwig Schmidt, Tsipras Dimitris, and Adrian Vladu. Towards deep learning models resistant to adversarial attacks. In *International Conference on Learning Representations (ICLR)*, 2018. [1](#), [2](#), [3](#), [4](#), [6](#), [11](#), [12](#)
- [23] Jan H. Metzen, Tim Genewein, Volker Fischer, and Bastian Bischoff. On Detecting Adversarial Perturbations. In *International Conference on Learning Representations (ICLR)*, 2017. [1](#)
- [24] Seyed-Mohsen Moosavi-Dezfooli, Alhussein Fawzi, and Pascal Frossard. Deepfool: A simple and accurate method to fool deep neural networks. In *IEEE Conference on Computer Vision and Pattern Recognition (CVPR)*, 2016. [1](#), [2](#), [6](#), [7](#)
- [25] Konda Reddy Mopuri, Aditya Ganeshan, and R. Venkatesh Babu. Generalizable Data-Free Objective for Crafting Universal Adversarial Perturbations. *IEEE Transactions on Pattern Analysis and Machine Intelligence (PAMI)*, 41(10):2452–2465, Oct. 2019. [2](#)
- [26] Konda Reddy Mopuri, Utsav Garg, and R Venkatesh Babu. Fast Feature Fool: A data independent approach to universal adversarial perturbations. In *Proceedings of the British Machine Vision Conference (BMVC)*, 2017. [2](#)
- [27] Nicolas Papernot, Patrick McDaniel, Somesh Jha, Matt Fredrikson, Z Berkay Celik, and Ananthram Swami. The limitations of deep learning in adversarial settings. In *IEEE European Symposium on Security and Privacy (EuroS&P)*, 2016. [1](#)
- [28] Nicolas Papernot, Patrick D. McDaniel, Ian J. Goodfellow, Somesh Jha, Z. Berkay Celik, and Ananthram Swami. Practical Black-Box Attacks against Deep Learning Systems using Adversarial Examples. In *Asia Conference on Computer and Communications Security (ASIACCS)*, 2017. [1](#)
- [29] Nicolas Papernot, Patrick D. McDaniel, Xi Wu, Somesh Jha, and Ananthram Swami. Distillation as a Defense to Adver-

- sarial Perturbations against Deep Neural Networks. *arXiv preprint arXiv:1511.04508*, 2015. [1](#)
- [30] Aditi Raghunathan, Jacob Steinhardt, and Percy Liang. Certified Defenses against Adversarial Examples. In *International Conference on Learning Representations (ICLR)*, 2018. [2](#)
- [31] Pouya Samangouei, Maya Kabkab, and Rama Chellappa. Defense-GAN: Protecting Classifiers Against Adversarial Attacks Using Generative Models. In *International Conference on Learning Representations (ICLR)*, 2018. [2](#)
- [32] Yang Song, Taesup Kim, Sebastian Nowozin, Stefano Ermon, and Nate Kushman. PixelDefend: Leveraging Generative Models to Understand and Defend against Adversarial Examples. In *International Conference on Learning Representations (ICLR)*, 2018. [2](#)
- [33] Nitish Srivastava, Geoffrey Hinton, Alex Krizhevsky, Ilya Sutskever, and Ruslan Salakhutdinov. Dropout: a simple way to prevent neural networks from overfitting. *The Journal of Machine Learning Research*, 15(56):1929–1958, 2014. [4](#)
- [34] Christian Szegedy, Wojciech Zaremba, Ilya Sutskever, Joan Bruna, Dumitru Erhan, Ian J. Goodfellow, and Rob Fergus. Intriguing properties of neural networks. In *International Conference on Learning Representations (ICLR)*, 2014. [1](#), [2](#)
- [35] Florian Tramèr, Alexey Kurakin, Nicolas Papernot, Dan Boneh, and Patrick McDaniel. Ensemble Adversarial Training: Attacks and Defenses. In *International Conference on Learning Representations (ICLR)*, 2018. [1](#), [2](#), [6](#), [12](#)
- [36] Eric Wong and J Zico Kolter. Provable defenses against adversarial examples via the convex outer adversarial polytope. *arXiv preprint arXiv:1711.00851*, 2017. [2](#)
- [37] Han Xiao, Kashif Rasul, and Roland Vollgraf. Fashion-MNIST: a novel image dataset for benchmarking machine learning algorithms. *arXiv preprint arXiv:1708.07747*, 2017. [5](#)
- [38] Cihang Xie, Jianyu Wang, Zhishuai Zhang, Zhou Ren, and Alan Yuille. Mitigating Adversarial Effects Through Randomization. In *International Conference on Learning Representations (ICLR)*, 2018. [2](#)
- [39] Sergey Zagoruyko and Nikos Komodakis. Wide Residual Networks. In *Proceedings of the British Machine Vision Conference (BMVC)*, 2016. [5](#), [13](#)
- [40] Hongyang Zhang, Yaodong Yu, Jiantao Jiao, Eric Xing, Laurent El Ghaoui, and Michael Jordan. Theoretically Principled Trade-off between Robustness and Accuracy. In *International Conference on Machine Learning (ICML)*, 2019. [1](#), [2](#), [6](#), [12](#)

Supplementary

S 1. Contents

- Section **S 2**: Network architecture.
- Section **S 3**: Adversarial training and Attack generation methods.
- Section **S 4**: Additional plots to illustrate over-fitting effect during single-step adversarial training.
- Section **S 5**: Effect of hyper-parameters
- Section **S 6**: Comparison with EAT
- Section **S 7**: Trend of R_e , training and validation loss during SADS.

S 2. Network Architecture

Network architecture of models used for MNIST and Fashion-MNIST datasets are shown in Table 7. Model-A and Model-B are used for generating adversarial samples in black-box setting.

S 3. Adversarial training and Attack generation methods

S 3.1. Adversarial Sample Generation Methods

In this subsection, we discuss the formulation of adversarial attacks.

Fast Gradient Sign Method (FGSM): Non-iterative attack method proposed by [13]. This method generates l_∞ norm bounded adversarial perturbation based on the linear approximation of loss function.

$$x^* = x + \epsilon \cdot \text{sign}(\nabla_x J(f(x; \theta), y_{true})) \quad (3)$$

Iterative Fast Gradient Sign Method (IFGSM) [17]: Iterative version of FGSM attack. At each iteration, adversarial perturbation of small step size (α) is added to the image. In our experiments, we set $\alpha = \epsilon / \text{steps}$.

$$\begin{aligned} x^0 &= x \\ x^{N+1} &= x^N + \alpha \cdot \text{sign}(\nabla_{x^N} J(f(x^N; \theta), y_{true})) \end{aligned} \quad (4)$$

Projected Gradient Descent (PGD) [22]: Initially, a small random noise sampled from Uniform distribution (U) is added to the image. Then at each iteration, perturbation of small step size (ϵ_{step}) is added to the image, and followed by re-projection.

$$\begin{aligned} x^0 &= x + U(-\epsilon_{step}, \epsilon_{step}, \text{shape}(x)) \\ x^{N+1} &= x^N + \epsilon_{step} \cdot \text{sign}(\nabla_{x^N} J(f(x^N; \theta), y_{true})) \\ x^{N+1} &= \text{clip}(x^{N+1}, \min = x - \epsilon, \max = x + \epsilon) \end{aligned} \quad (6)$$

Momentum Iterative Fast Gradient Sign Method (MI-FGSM) [10]: Introduces a momentum term into the IFGSM formulation. Here, μ represents the momentum term. α represents step size and is set to ϵ / steps .

$$\begin{aligned} x^0 &= x \\ g^{N+1} &= \mu \cdot g^N + \frac{\nabla_{x^N} J(f(x^N; \theta), y_{true})}{\|\nabla_{x^N} J(f(x^N; \theta), y_{true})\|_1} \\ x^{N+1} &= x^N + \alpha \cdot \text{sign}(g^{N+1}) \end{aligned} \quad (9)$$

S 3.2. Adversarial Training Methods

In this subsection we explain the existing adversarial training methods.

Table 7: Architecture of networks used for MNIST and Fashion-MNIST datasets.

LeNet+	Model-A	Model-B	Model-C	Model-D
Conv(32,5,5) + Relu MaxPool(2,2)	Conv(64,5,5) + Relu Conv(64,5,5) + Relu	Dropout(0.2) Conv(64,8,8) + Relu	Conv(128,3,3) + Tanh MaxPool(2,2)	$\left\{ \begin{array}{l} \text{FC}(300) + \text{Relu} \\ \text{Dropout}(0.5) \end{array} \right\} \times 4$ FC + Softmax
Conv(64,5,5) + Relu MaxPool(2,2)	Dropout(0.25) FC(128) + Relu	Conv(128,6,6) + Relu Conv(128,5,5) + Relu	Conv(64,3,3) + Tanh MaxPool(2,2)	
FC(1024) + Relu	Dropout(0.5)	Dropout(0.5)	FC(128) + Relu	
FC + Softmax	FC + Softmax	FC + Softmax	FC + Softmax	

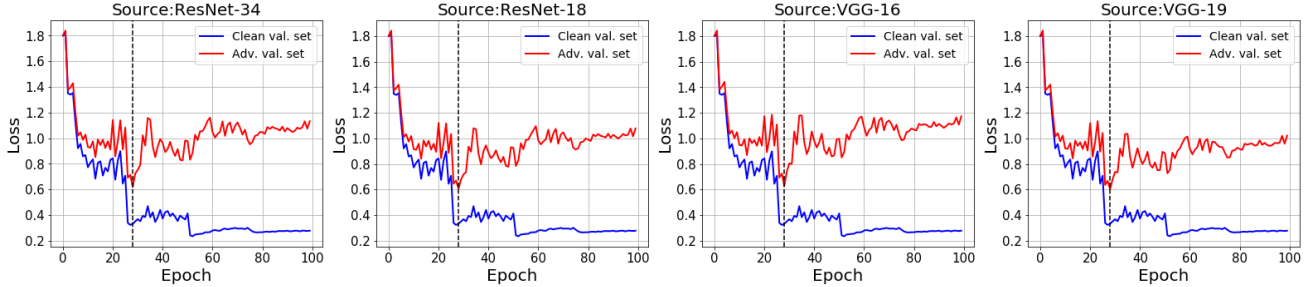


Figure 6: **Single-step adversarial training:** Trend of validation loss during single-step adversarial training, obtained for ResNet-34 trained on CIFAR-10 dataset. Adversarial validation set is generated using column-1: ResNet-34, column-2: ResNet-18, column-3: VGG-16 and column-4: VGG-19.

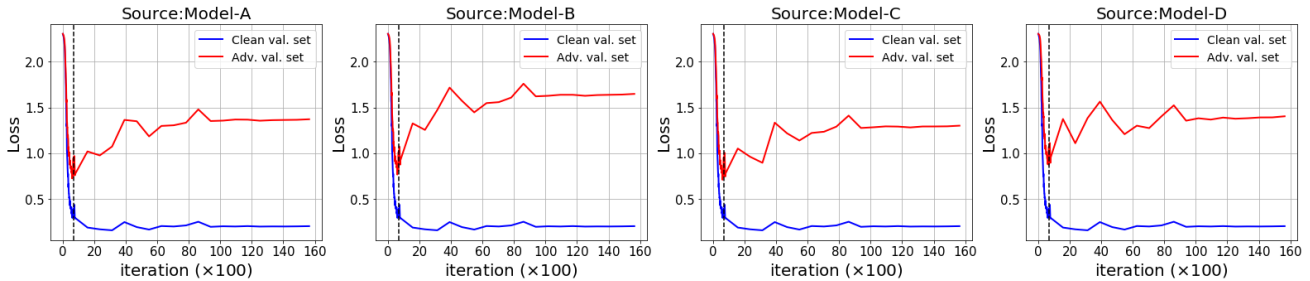


Figure 7: **Single-step adversarial training:** Trend of validation loss during single-step adversarial training, obtained for LeNet+ trained on MNIST dataset. Adversarial validation set is generated using column-1: Model-A, column-2: Model-B, column-3: Model-C and column-4: Model-D.

FGSM Adversarial Training (FAT): During training, at each iteration a portion of clean samples in the mini-batch are replaced with their corresponding adversarial samples generated using the model being trained. Fast Gradient Sign Method (FGSM) is used for generating these adversarial samples.

Ensemble Adversarial Training (EAT) [35]: At each iteration a portion of clean samples in the mini-batch are replaced with their corresponding adversarial samples. These adversarial samples are generated by the model being trained or by one of the model from the fixed set of pre-trained models. Table 8 shows the setup used for EAT method.

PGD Adversarial Training (PAT): Multi-step adversarial training method proposed by [22]. At each iteration all the clean samples in the mini-batch are replaced with their corresponding adversarial samples generated using the model being trained. Projected Gradient Descent (PGD) method is used for generating these samples.

TRADES: Multi-step adversarial training method proposed by [40]. The method proposes a regularizer that encourages the output of the network to be smooth. The training mini-batches contain clean and their corresponding adversarial samples. These adversarial samples are generated using Projected Gradient Descent with modified loss function.

S 4. Additional plots to illustrate over-fitting effect

In the main paper, we showed over-fitting effect during training of LeNet+ on MNIST dataset using single-step adversarial training. Fig. 6 shows the plot of validation loss, obtained for ResNet-34 trained on CIFAR-10 dataset using single-step adversarial training. We observe over-fitting effect even when model with different architecture is used for generating adversarial validation set. Fig. 7 shows the validation loss obtained for LeNet+ trained on MNIST dataset using single-step adversarial training. Normally trained models with different architecture are used for generating adversarial validation set.

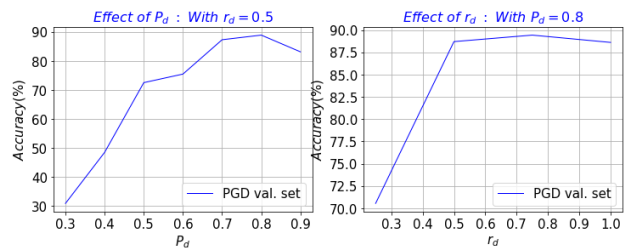


Figure 8: Effect of hyper-parameter P_d and r_d of SADS

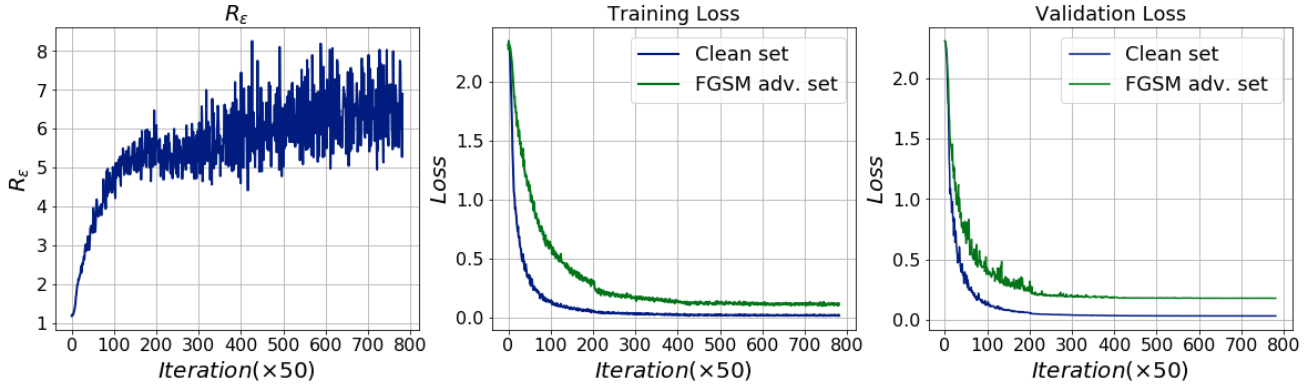


Figure 9: **MNIST**: Trend of R_ϵ , training loss, and validation loss during SADS training method, obtained for LeNet+ trained on MNIST dataset. Column-1: plot of R_ϵ versus iteration. Column-2: training loss versus iteration. Column-3: validation loss versus iteration. Note that, for the entire training duration R_ϵ does not decay, and no over-fitting effect can be observed.

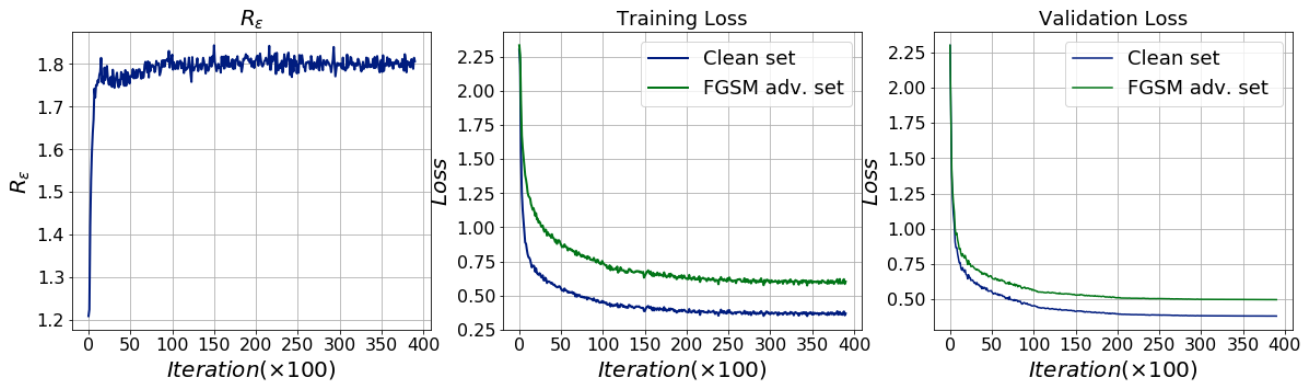


Figure 10: **Fashion-MNIST**: Trend of R_ϵ , training loss, and validation loss during SADS training method, obtained for LeNet+ trained on Fashion-MNIST dataset. Column-1: plot of R_ϵ versus iteration. Column-2: training loss versus iteration. Column-3: validation loss versus iteration. Note that, for the entire training duration R_ϵ does not decay, and no over-fitting effect can be observed.

S 5. Effect of Hyper-Parameters

In order to show the effect of hyper-parameters, we train LeNet+ shown in table 7 on MNIST dataset, using SADS with different hyper-parameter settings. Validation set accuracy of the model for PGD attack ($\epsilon = 0.3$ and $steps = 40$) is obtained for each hyper-parameter setting with one of them being fixed and the other being varied.

Effect of hyper-parameter P_d : The hyper-parameter P_d defines the initial dropout probability applied to all dropout layers. We train LeNet+ on MNIST dataset, using the proposed method for different initial dropout probability P_d . Column-1 of Fig. 8 shows the effect of varying dropout probability from 0.3 to 0.9. It can be observed that the robustness of the model to multi-step attack initially increases with the increase in the value of P_d ($P_d < 0.8$), and further increase in P_d causes the model’s robustness to decrease, and this is due to under-fitting.

Effect of hyper-parameter r_d : The hyper-parameter r_d decides the iteration at which dropout probability reaches zero

and is expressed in terms of maximum training iteration. Column-2 of Fig. 8 shows the effect varying r_d from 1/4 to 1. It can be observed that for $r_d < 0.5$, there is degradation in the robustness of the model against multi-step attacks. This is because, during the initial stages of training, learning rate is high and the model can easily over-fit to adversaries generated by single-step method.

S 6. Comparison with Ensemble Adversarial Training

We train WideResNet-28-10 [39] on CIFAR-10 [16] dataset using EAT and SADS. Table 8 shows the setup used for EAT. Pre-trained models are used for generating adversarial samples during EAT. Table 9 shows the recognition accuracy of models trained using EAT and SADS in white-box attack setting. It can be observed that the model trained using SADS is robust to both single-step (FGSM) and multi-step attacks (PGD), whereas models trained using EAT are susceptible to multi-step attack.

S 7. SADS: Trend of R_ϵ , training and validation loss

Fig. 9 and 10 show the trend of R_ϵ , training and validation loss, obtained for models trained using SADS. It can be observed that for the entire training duration R_ϵ does not decay and no over-fitting effect can be observed.

Table 8: Setup used for Ensemble Adversarial Training.

	Network to be trained	Pre-trained Models
CIFAR-10	WRN-28-10 (Ens-A)	WRN-28-10, ResNet-34
	WRN-28-10 (Ens-B)	WRN-28-10, VGG-19
	WRN-28-10 (Ens-C)	ResNet-34, VGG-19

Table 9: **CIFAR-10: White-Box attack.** Classification accuracy (%) of models trained on CIFAR-10 dataset using different training methods. For all attacks $\epsilon=8/255$ is used and for PGD attack $\epsilon_{step}=2/255$ and $steps=7$ is used.

Training Method	Attack Method		
	Clean	FGSM	PGD-7
EAT Ens-A	92.92	59.56	19.21
EAT Ens-B	92.75	63.40	5.34
EAT Ens-C	93.11	59.74	12.03
SADS	82.01 ± 0.06	51.99 ± 1.02	45.66 ± 1.26